

Neutrino phenomenology in a model with generalized CP symmetry within type-I seesaw framework

Tapender,^{1,†} Sanjeev Kumar,^{2,‡} and Surender Verma^{1,*}

¹*Department of Physics and Astronomical Science,
Central University of Himachal Pradesh, Dharamshala-176215, India*

²*Department of Physics and Astrophysics, University of Delhi, Delhi-110007, India*

 (Received 11 September 2023; accepted 6 December 2023; published 25 January 2024)

We investigate the consequences of generalized CP (GCP) symmetry within the context of the two Higgs doublet model (2HDM), specifically focusing on the lepton sector. Utilizing the type-I seesaw framework, we study an intriguing connection between the Dirac Yukawa couplings originating from both Higgs fields, leading to a reduction in the number of independent Yukawa couplings and simplifying the scalar and Yukawa sectors when compared to the general 2HDM. The constraints coming from CP symmetry of class three (CP3) results in two right-handed neutrinos having equal masses and leads to a diagonal right-handed Majorana neutrino mass matrix. Notably, CP symmetry experiences a soft breaking due to the phase associated with the vacuum expectation value of the second Higgs doublet. The model aligns well with observed charged lepton masses and neutrino oscillation data, explaining both masses and mixing angles, and yields distinct predictions for normal and inverted neutrino mass hierarchies. It features a novel interplay between atmospheric mixing angle θ_{23} and neutrino mass hierarchy: The angle θ_{23} is below maximal for the normal hierarchy and above maximal for inverted hierarchy. Another interesting feature of the model is inherent CP violation for the inverted hierarchy.

DOI: [10.1103/PhysRevD.109.015004](https://doi.org/10.1103/PhysRevD.109.015004)

I. INTRODUCTION

The standard model (SM) of particle physics provides a unified and well-tested theoretical framework for explaining the interactions of known fundamental particles. It explains how quarks and charged leptons acquire mass. However, it cannot account for the nonzero mass of neutrinos, which is necessary to explain observed neutrino oscillations. One way to explain nonzero neutrino masses is by introducing SU(2) singlet right-handed neutrinos into the particle content of the SM and allowing them to have a Dirac mass term. However, this leads to a very small Yukawa coupling $\mathcal{O}(\approx 10^{-12})$ to explain smallness of the neutrino masses. To address this issue, in addition to the Dirac mass term, one can introduce another mass term by utilizing the right-handed neutrinos and their charge-conjugated fields. This additional term is known as the Majorana mass term, which violates lepton number.

Since the masses of these right-handed neutrinos do not arise due to the Higgs mechanism, they can be very heavy $\mathcal{O}(10^{15})$ GeV. This, in turn, results in the left-handed neutrinos being light, thereby accounting for the smallness of the neutrino masses. This mechanism of neutrino mass generation is referred to as the Type-I seesaw [1–5].

Extending beyond the Standard Model (SM), a natural step involves adding another Higgs doublet, known as the two Higgs doublet model (2HDM). Initially proposed to address matter-antimatter asymmetry alongside the quark mixing matrix [6], the 2HDM doesn't explain neutrino mass. The vacuum expectation values of these two SU(2) doublets spontaneously break the CP symmetry contributing as an extra source for generating matter-antimatter asymmetry [6]. Further, the need for a second Higgs doublet arises naturally in the minimal supersymmetric standard model (MSSM) [7] and axion models [8,9]. Another reason for considering 2HDM is that it preserves the ρ parameter [6], connecting the mechanism of electroweak symmetry breaking with the masses of SM gauge bosons [10].

Despite these characteristic features, 2HDMs have shortcomings, including the inability to explain neutrino mass, dark matter, and the allowance of tree-level flavor changing neutral currents (FCNC). The presence of FCNC arises because both SU(2) scalar doublets can couple to fermions. However, there are studies suggesting mechanisms to mitigate FCNC interactions. For example:

*Corresponding author: s_7verma@hpcu.ac.in

†tapenderphy@gmail.com

‡skverma@physics.du.ac.in

Published by the American Physical Society under the terms of the Creative Commons Attribution 4.0 International license. Further distribution of this work must maintain attribution to the author(s) and the published article's title, journal citation, and DOI. Funded by SCOAP³.

- (1) FCNC interactions can be fine-tuned by carefully selecting Yukawa couplings that are suppressed by the heavy mass of the scalar boson responsible for FCNC [11].
- (2) FCNC can be eliminated by employing a global symmetry, such as Z_2 , which restricts a given scalar boson from coupling to fermions of different electric charges [12,13].
- (3) Tree-level FCNC can be eliminated by using a global $U(1)$ Peccei-Quinn symmetry [14].

In addition to addressing FCNC, there have been various attempts to enhance 2HDMs to incorporate neutrino masses [15–20] and dark matter [21–26].

However, 2HDM poses a challenge due to its large number of free parameters, making it difficult to probe through collider experiments like the LHC. In general, the scalar potential of the 2HDM consists of 14 parameters and can exhibit CP conserving or CP violating behavior [11,27]. Consequently, additional constraints are necessary, often derived from symmetry arguments, to establish relationships among these parameters.

The study of generalized CP (GCP) transformations [28–30] within the scalar sector of 2HDM is an example of imposing additional symmetries [31,32]. GCP transformations can be categorized in various ways. In Ref. [31], they are classified into three categories: CP1, CP2, and CP3. CP1 and CP2 correspond to discrete transformations, while CP3 is a continuous transformation that can be extended to the fermionic sector [32], and they have applied this to the quark sector. Furthermore, the CP symmetries of the scalar sector in the 2HDM have been thoroughly investigated using the basis invariant bilinear formalism [33–38] in many works [34–37].

The idea of implementing GCP symmetry to obtain the lepton mixing parameters is widely recognized. GCP symmetry has been used in various models in combination with the flavor symmetry of the leptons to obtain the lepton mixing parameters and to explain CP violation [39–46]. There are models that use the concept of remnant CP symmetries to obtain the lepton mixing parameters [47–51]. The use of multiple Higgs formalism is common in supersymmetry (SUSY) models. Many attempts have been made to explain the neutrino data in SUSY models [52–57]. Apart from SUSY, there are also beyond the Standard Model (BSM) neutrino mass models with two Higgs doublets, which use some symmetry, such as Z_2 , to constrain their Yukawa couplings and hence the parameter space [15–26]. In our work, we have used GCP symmetry to study the implications of GCP on neutrino phenomenology and to study CP violation. In particular, we've extended CP3 to the 2HDM's leptonic Yukawa sector, introducing CP violation through the second Higgs's v_{ev} phase. Neutrino masses are generated *via* the Type-I seesaw relation involving right-handed neutrinos.

The paper is structured as follows: In Sec. II, we present the basic formalism of 2HDM. Section III elaborates on

extending CP3 to the neutrino Yukawa sector within the Type-I seesaw mechanism. We discuss our numerical analysis in Sec. IV. Finally, in Sec. V, we summarize our conclusions.

II. TWO HIGGS DOUBLET MODEL UNDER GENERALIZED CP SYMMETRY

In 2HDMs, the Standard Model's field content enlarges with the addition of an extra Higgs doublet, denoted as Φ_2 , which possesses the same charge assignments as the Higgs field in the SM. However, this minimal expansion in the scalar sector results in an increased number of free parameters. To address this parameter growth, it becomes imperative to introduce specific symmetries. In this context, the generalized CP (GCP) symmetry is considered. Under GCP, scalar doublets undergo transformations as elucidated in [31]:

$$\Phi_a \rightarrow \Phi_a^{\text{GCP}} = X_{aa} \Phi_a^*, \quad (1)$$

where X is an arbitrary unitary CP transformation matrix.

There always exists a choice of basis for which most general GCP transformation matrix can be brought to the form [58]

$$X = \begin{pmatrix} \cos \theta & \sin \theta \\ -\sin \theta & \cos \theta \end{pmatrix}, \quad (2)$$

where $0 \leq \theta \leq \pi/2$. So, we have three distinct classes with respect to the parameter θ as mentioned in [31]:

- (1) When $\theta = 0$, the symmetry is referred to as CP symmetry of class one (CP1).
- (2) For $\theta = \pi/2$, the symmetry is known as CP symmetry of class two (CP2).
- (3) In the range $0 < \theta < \pi/2$, the symmetry is labeled as CP symmetry of class three (CP3), and importantly it constitutes a continuous symmetry.

The most general scalar potential with two Higgs doublets can be written as

$$\begin{aligned} V_H = & m_{11}^2 \Phi_1^\dagger \Phi_1 + m_{22}^2 \Phi_2^\dagger \Phi_2 - [m_{12}^2 \Phi_1^\dagger \Phi_2 + \text{H.c.}] \\ & + \frac{1}{2} \lambda_1 (\Phi_1^\dagger \Phi_1)^2 + \frac{1}{2} \lambda_2 (\Phi_2^\dagger \Phi_2)^2 \\ & + \lambda_3 (\Phi_1^\dagger \Phi_1) (\Phi_2^\dagger \Phi_2) + \lambda_4 (\Phi_1^\dagger \Phi_2) (\Phi_2^\dagger \Phi_1) \\ & + \left[\frac{1}{2} \lambda_5 (\Phi_1^\dagger \Phi_2)^2 + \lambda_6 (\Phi_1^\dagger \Phi_1) (\Phi_1^\dagger \Phi_2) \right. \\ & \left. + \lambda_7 (\Phi_2^\dagger \Phi_2) (\Phi_1^\dagger \Phi_2) + \text{H.c.} \right], \quad (3) \end{aligned}$$

having total 14 parameters. Here, m_{11}^2 , m_{22}^2 and λ_1 through λ_4 are real parameters, while m_{12}^2 , λ_5 , λ_6 and λ_7 are generally complex.

Based on the findings in Refs. [31,32], it is established that, in addition to the standard CP symmetry $CP1$, $CP3$ is the only symmetry that can be extended to the Yukawa sector for leptons. To maintain $CP3$ invariance within the scalar potential, certain conditions must be satisfied. Specifically, we must have $m_{11}^2 = m_{22}^2$, $m_{12}^2 = 0$, $\lambda_2 = \lambda_1$, $\lambda_6 = 0$, $\lambda_7 = 0$, and $\lambda_5 = \lambda_1 - \lambda_3 - \lambda_4$, which must be a real parameter.

To avoid the presence of Goldstone bosons following spontaneous symmetry breaking, it is necessary to introduce soft $CP3$ symmetry breaking. Therefore, we will consider $m_{11}^2 \neq m_{22}^2$ and $\Re[m_{12}^2] \neq 0$. This softly broken $CP3$ symmetric potential also leads to a CP -violating vacuum expectation value (VEV) for the second Higgs doublet, which assumes a crucial role in the exploration of CP violation in the lepton sector, as we will delve into in the upcoming sections.

III. CP3 IN YUKAWA SECTOR WITH TYPE-I SEESAW

In our study, we have extended the SM with the addition of second Higgs doublet ϕ_2 and three right-handed neutrinos denoted as N_R . Within the framework of the Type-I seesaw mechanism, the relevant Yukawa Lagrangian responsible for generating the masses of both charged leptons and neutrinos¹ is expressed as follows

$$-\mathcal{L}_Y = \bar{L}_L \Gamma_a \Phi_a l_R + \bar{L}_L Y_a \tilde{\Phi}_a N_R + \frac{1}{2} \bar{N}_R^c M N_R + \text{H.c.}, \quad (4)$$

where L_L , l_R are Standard Model $SU(2)$ left-handed doublets and right-handed singlets, Φ_a ($a = 1, 2$) are Higgs doublets, and N_R are right-handed neutrino singlets. Γ_a and Y_a are the Yukawa coupling matrices for charged leptons and neutrinos, respectively, and M is lepton number violating Majorana mass term for right-handed neutrinos. Now we will extend the GCP symmetry to the leptonic Yukawa sector.

The fields involved in Eq. (4) transforms under GCP symmetry as

$$\left. \begin{aligned} \Phi_a &\rightarrow \Phi_a^{\text{GCP}} = X_{ab} \Phi_b^*, \\ \tilde{\Phi}_a &\rightarrow \tilde{\Phi}_a^{\text{GCP}} = X_{ab}^* (\Phi_b^\dagger)^T, \\ L_L &\rightarrow L_L^{\text{GCP}} = iX_\zeta \gamma^0 C \bar{L}_L^T, \\ l_R &\rightarrow l_R^{\text{GCP}} = iX_\beta \gamma^0 C \bar{l}_R^T, \\ N_R &\rightarrow N_R^{\text{GCP}} = iX_\gamma \gamma^0 C \bar{N}_R^T, \end{aligned} \right\}, \quad (5)$$

where γ^0 is Dirac gamma matrix, and C is charge conjugation matrix, and X , X_ζ , X_β , and X_γ are CP transformation matrices.

For Lagrangian to remain invariant under these CP transformations, we find Yukawa coupling matrices to transform as

$$\Gamma_b^* = X_\zeta^\dagger \Gamma_a X_\beta X_{ab}, \quad (6)$$

$$Y_b^* = X_\zeta^\dagger Y_a X_\gamma X_{ab}^*, \quad (7)$$

and Majorana mass matrix to transform as

$$M^* = X_\gamma^T M X_\gamma, \quad (8)$$

where

$$M = \begin{pmatrix} M_{11} & M_{12} & M_{13} \\ M_{12} & M_{22} & M_{23} \\ M_{13} & M_{23} & M_{33} \end{pmatrix}. \quad (9)$$

The CP transformation matrices involved are given by

$$X_\zeta = \begin{pmatrix} \cos \zeta & \sin \zeta & 0 \\ -\sin \zeta & \cos \zeta & 0 \\ 0 & 0 & 1 \end{pmatrix}, \quad (10)$$

$$X_\beta = \begin{pmatrix} \cos \beta & \sin \beta & 0 \\ -\sin \beta & \cos \beta & 0 \\ 0 & 0 & 1 \end{pmatrix}, \quad (11)$$

$$X_\gamma = \begin{pmatrix} \cos \gamma & \sin \gamma & 0 \\ -\sin \gamma & \cos \gamma & 0 \\ 0 & 0 & 1 \end{pmatrix}. \quad (12)$$

It was found in Ref. [32] that $CP3$ symmetry with $\theta = \pi/3$ ($\zeta = \beta = \gamma = \pi/3$) can be extended to Yukawa sector producing correct quark masses. Under these conditions, the forms of Yukawa coupling matrices given in Eqs. (6) and (7) become

$$\left. \begin{aligned} \Gamma_1 &= \begin{pmatrix} ia_{11} & ia_{12} & a_{13} \\ ia_{12} & -ia_{11} & a_{23} \\ a_{31} & a_{32} & 0 \end{pmatrix}, \\ \Gamma_2 &= \begin{pmatrix} ia_{12} & -ia_{11} & -a_{23} \\ -ia_{11} & -ia_{12} & a_{13} \\ -a_{32} & a_{31} & 0 \end{pmatrix}, \\ Y_1 &= \begin{pmatrix} ib_{11} & ib_{12} & b_{13} \\ ib_{12} & -ib_{11} & b_{23} \\ b_{31} & b_{32} & 0 \end{pmatrix}, \\ Y_2 &= \begin{pmatrix} ib_{12} & -ib_{11} & -b_{23} \\ -ib_{11} & -ib_{12} & b_{13} \\ -b_{32} & b_{31} & 0 \end{pmatrix}, \end{aligned} \right\}, \quad (13)$$

¹For quark masses, see Ref. [32].

where all a 's and b 's are real parameters. The choice of $\theta = \pi/3$ alongside $\zeta = \beta = \gamma = \pi/3$ in the leptonic sector stems from the similarity in GCP transformation properties between quarks and leptonic fields, as outlined in Eq. (5).

Now, we need to solve constraints given by Eq. (8), which can be rewritten as

$$M^* - X_\gamma^T M X_\gamma = 0. \quad (15)$$

Using Eqs. (9) and (12) in Eq. (15), the set of constraints are

$$M_{11}^* - M_{11} \cos^2 \gamma - M_{22} \sin^2 \gamma + M_{12} \sin 2\gamma = 0, \quad (16)$$

$$M_{12}^* - M_{12} \cos 2\gamma + (-M_{11} + M_{22}) \sin \gamma \cos \gamma = 0, \quad (17)$$

$$M_{22}^* - M_{22} \cos^2 \gamma - 2M_{12} \cos \gamma \sin \gamma - M_{11} \sin^2 \gamma = 0, \quad (18)$$

$$M_{13}^* - M_{13} \cos \gamma + M_{23} \sin \gamma = 0, \quad (19)$$

$$M_{23}^* - M_{23} \cos \gamma - M_{13} \sin \gamma = 0, \quad (20)$$

$$M_{33}^* - M_{33} = 0. \quad (21)$$

In Eqs. (16), (17), and (18), the real part can be separated out as

$$\begin{pmatrix} 1 - \cos^2 \gamma & \sin 2\gamma & -\sin^2 \gamma \\ -\cos \gamma \sin \gamma & 1 - \cos 2\gamma & \cos \gamma \sin \gamma \\ -\sin^2 \gamma & -2\cos \gamma \sin \gamma & 1 - \cos^2 \gamma \end{pmatrix} \begin{pmatrix} \Re[M_{11}] \\ \Re[M_{12}] \\ \Re[M_{22}] \end{pmatrix} = 0, \quad (22)$$

and the imaginary part can be separated out as

$$\begin{pmatrix} -1 - \cos^2 \gamma & \sin 2\gamma & -\sin^2 \gamma \\ -\cos \gamma \sin \gamma & -1 - \cos 2\gamma & \cos \gamma \sin \gamma \\ -\sin^2 \gamma & -2\cos \gamma \sin \gamma & -1 - \cos^2 \gamma \end{pmatrix} \begin{pmatrix} \Im[M_{11}] \\ \Im[M_{12}] \\ \Im[M_{22}] \end{pmatrix} = 0. \quad (23)$$

Further, from Eqs. (19) and (20) we have, for real part,

$$\begin{pmatrix} 1 - \cos \gamma & \sin \gamma \\ -\sin \gamma & 1 - \cos \gamma \end{pmatrix} \begin{pmatrix} \Re[M_{13}] \\ \Re[M_{23}] \end{pmatrix} = 0, \quad (24)$$

and, for imaginary part,

$$\begin{pmatrix} -1 - \cos \gamma & \sin \gamma \\ -\sin \gamma & -1 - \cos \gamma \end{pmatrix} \begin{pmatrix} \Im[M_{13}] \\ \Im[M_{23}] \end{pmatrix} = 0. \quad (25)$$

For $\gamma = \pi/3$, we have

$$\begin{pmatrix} \frac{3}{4} & \frac{\sqrt{3}}{2} & \frac{-3}{4} \\ -\frac{\sqrt{3}}{4} & \frac{3}{2} & \frac{\sqrt{3}}{4} \\ \frac{-3}{4} & \frac{-\sqrt{3}}{2} & \frac{3}{4} \end{pmatrix} \begin{pmatrix} \Re[M_{11}] \\ \Re[M_{12}] \\ \Re[M_{22}] \end{pmatrix} = 0, \quad (26)$$

$$\begin{pmatrix} \frac{-5}{4} & \frac{\sqrt{3}}{2} & \frac{-3}{4} \\ -\frac{\sqrt{3}}{4} & -\frac{1}{2} & \frac{\sqrt{3}}{4} \\ \frac{-3}{4} & -\frac{\sqrt{3}}{2} & -\frac{5}{4} \end{pmatrix} \begin{pmatrix} \Im[M_{11}] \\ \Im[M_{12}] \\ \Im[M_{22}] \end{pmatrix} = 0, \quad (27)$$

and

$$\begin{pmatrix} \frac{1}{2} & \frac{\sqrt{3}}{2} \\ -\frac{\sqrt{3}}{2} & \frac{1}{2} \end{pmatrix} \begin{pmatrix} \Re[M_{13}] \\ \Re[M_{23}] \end{pmatrix} = 0, \quad (28)$$

$$\begin{pmatrix} -\frac{3}{2} & \frac{\sqrt{3}}{2} \\ -\frac{\sqrt{3}}{2} & -\frac{3}{2} \end{pmatrix} \begin{pmatrix} \Im[M_{13}] \\ \Im[M_{23}] \end{pmatrix} = 0. \quad (29)$$

In Eqs. (27), (28), and (29), the determinant of the square matrix is nonzero, implying a unique solution where $\Im[M_{11}]$, $\Im[M_{12}]$, $\Im[M_{22}]$, $\Re[M_{13}]$, $\Re[M_{23}]$, $\Im[M_{13}]$, and $\Im[M_{23}]$ all equal zero. On the other hand, in Eq. (26), the determinant of the square matrix is zero, indicating arbitrary solutions, with $\Re[M_{12}]$ equal to zero and $\Re[M_{11}] \equiv M_1$ equal to $\Re[M_{22}]$. Furthermore, Eq. (21) leads to $\Im[M_{33}]$ being zero, leaving only $\Re[M_{33}] \equiv M_3$ as the relevant parameter.

It is worth noting that the CP3 constraint results in two right-handed neutrinos having equal masses, leading to a diagonal matrix M , described as follows:

$$M = \begin{pmatrix} M_1 & 0 & 0 \\ 0 & M_1 & 0 \\ 0 & 0 & M_3 \end{pmatrix}. \quad (30)$$

After spontaneous symmetry breaking (SSB), both Higgs doublets get VEVs, given by

$$\langle \Phi_1 \rangle = \begin{pmatrix} 0 \\ \frac{v_1}{\sqrt{2}} \end{pmatrix}, \quad \langle \Phi_2 \rangle = \begin{pmatrix} 0 \\ e^{i\alpha} \frac{v_2}{\sqrt{2}} \end{pmatrix}, \quad (31)$$

with condition that $v = \sqrt{v_1^2 + v_2^2} \approx 245$ GeV, where v is the standard model VEV. Consequently, the charged leptons mass matrix becomes

$$M_l = \frac{1}{\sqrt{2}} (v_1 \Gamma_1 + e^{i\alpha} v_2 \Gamma_2), \quad (32)$$

$$= \frac{1}{\sqrt{2}} (\cos \phi \Gamma_1 + e^{i\alpha} \sin \phi \Gamma_2) v, \quad (33)$$

and for neutrinos we have the Dirac mass matrix given by

$$M_D = \frac{1}{\sqrt{2}} (v_1 Y_1 + e^{-i\alpha} v_2 Y_2), \quad (34)$$

$$= \frac{1}{\sqrt{2}} (\cos \phi Y_1 + e^{-i\alpha} \sin \phi Y_2) v, \quad (35)$$

where ϕ is defined as $\tan \phi = v_2/v_1$.

The charged lepton mass matrix can be diagonalized as

$$M_l = U_l m_{\text{diag}} U_l^\dagger, \quad (36)$$

where U_l and U_R are 3×3 unitary matrices, and $m_{\text{diag}} = \text{diag}(m_e, m_\mu, m_\tau)$ is diagonal matrix with positive real entries giving mass eigenvalues of electron, muon, and tau, respectively. So, we have

$$U_l^\dagger M_l M_l^\dagger U_l = m_{\text{diag}}^2. \quad (37)$$

In order to work in the basis wherein the charged lepton mass matrix is diagonal, we use the matrix U_l to rotate M_D into the required basis; i.e.,

$$M_D^{\text{new}} = U_l^\dagger M_D. \quad (38)$$

Using Type-I seesaw, the effective light neutrinos mass matrix is given by

$$M_\nu = -M_D^{\text{new}} M^{-1} (M_D^{\text{new}})^T, \quad (39)$$

$$= -(U_l^\dagger M_D) M^{-1} (U_l^\dagger M_D)^T, \quad (40)$$

which is a complex symmetric matrix. This matrix is related to Yukawa coupling matrices Y_1 and Y_2 through Eq. (35). The effective light neutrino mass matrix can be diagonalized by 3×3 unitary matrix U as

$$U^\dagger M_\nu U^* = m, \quad (41)$$

where $m_{ik} = m_i \delta_{ik}$, $m_i > 0$ ($i, k = 1, 2, 3$).

We will now move forward with the numerical determination of charged lepton masses and the parameters governing neutrino oscillations. This process entails the variation of free parameters to ascertain the permissible parameter space within the model.

IV. NUMERICAL ANALYSIS AND DISCUSSION

In our numerical analysis, we generated random numbers uniformly for the VEV-phase α in the range of 0 to 2π . We also generated random numbers uniformly for the masses of the right-handed neutrinos M_1 and M_3 , which ranged from 10^{11} to 10^{13} GeV and from 1.1×10^{13} to 10^{15} GeV, respectively. We considered two cases for the VEV v_1 , as discussed in the following subsections.

A. When $v_1 \ll v_2$

In this scenario, we examined the influence of a very small VEV on our parameter space. To emphasize the dominance of VEV v_2 , we randomly varied v_1 in the range of $(0 - 5) \times 10^{-6}$ GeV. The value of v_2 is subsequently determined using the equation $v_2 = \sqrt{v^2 - v_1^2}$ GeV. We then determined the masses of charged leptons and the

TABLE I. The ranges of Yukawa couplings used in numerical analysis for charged leptons.

Yukawa coupling parameter	When $v_1 \ll v_2$ range	When v_1 ranges from (10–17) GeV range
a_{11}	$3 \times 10^{-5} - 6 \times 10^{-5}$	$2 \times 10^{-5} - 3 \times 10^{-5}$
a_{12}	$8 \times 10^{-5} - 1 \times 10^{-4}$	$6 \times 10^{-5} - 8 \times 10^{-5}$
a_{13}	$6 \times 10^{-3} - 8 \times 10^{-3}$	$6 \times 10^{-3} - 7 \times 10^{-3}$
a_{23}	$6 \times 10^{-3} - 8 \times 10^{-3}$	$8 \times 10^{-3} - 9 \times 10^{-3}$
a_{31}	$4 \times 10^{-4} - 6 \times 10^{-4}$	$4 \times 10^{-4} - 6 \times 10^{-4}$
a_{32}	$1 \times 10^{-4} - 2 \times 10^{-4}$	$1 \times 10^{-4} - 2 \times 10^{-4}$

parameters governing neutrino oscillations, which we discuss in the following subsections.

1. Charged lepton masses

To compute the masses of charged leptons, we varied the Yukawa coupling parameters within the range specified in Table I. We then proceeded to numerically diagonalize the mass matrix $M_l M_l^\dagger$, as described in Eq. (37), to obtain the squared masses of charged leptons (m_e^2, m_μ^2, m_τ^2). Through this analysis, we identified parameter values that consistently yielded the correct charged lepton masses for both normal ($m_1 < m_2 < m_3$) and inverted ($m_3 < m_1 < m_2$) hierarchies of neutrinos. The benchmark points are listed in the second column of Table II. With these parameter values, we calculated the charged lepton masses, as presented in Table III, which closely align with experimentally observed values.

2. Neutrino oscillation parameters

To find the neutrino mixing angles and mass-squared differences, we first rotated the neutrino mass matrix using the previously derived U_l . The matrix M_ν , described in Eq. (40), generally contains Yukawa couplings Y_1 and Y_2 , as given in Eq. (14). We then introduced random variations

TABLE II. Benchmark points for both the cases (i) $v_1 \ll v_2$ (second column) (ii) v_1 ranges from (10–17) GeV (third column), yielding correct values of charged lepton masses.

Parameters (Units)	When v_1 ranges from (10–17) GeV		
	When $v_1 \ll v_2$	NH	IH
a_{11}	5.740882×10^{-5}	2.692411×10^{-5}	2.692412×10^{-5}
a_{12}	9.066478×10^{-5}	7.993756×10^{-5}	7.993757×10^{-5}
a_{13}	7.124930×10^{-3}	6.382725×10^{-3}	6.382726×10^{-3}
a_{23}	7.377109×10^{-3}	8.028028×10^{-3}	8.028028×10^{-3}
a_{31}	5.843790×10^{-4}	5.945601×10^{-4}	5.945602×10^{-4}
a_{32}	1.377038×10^{-4}	1.065540×10^{-4}	1.065540×10^{-4}
v_1 (GeV)	3.287415×10^{-6}	11.00	15.30
v_2 (GeV)	245	244.75	244.52
α (°)	197.54	177.68	170.20

TABLE III. The values of the charged lepton masses obtained using benchmark points given in Table II.

Masses (MeV)	When	When v_1 ranges from (10–17) GeV	
	$v_1 \ll v_2$	NH	IH
m_e	0.510	0.511	0.511
m_μ	105.66	105.66	105.66
m_τ	1776.87	1776.85	1776.85

to these Yukawa coupling parameters within the specified ranges presented in the second column of Table IV, considering both normal (NH) and inverted (IH) hierarchies. This process allowed us to identify a benchmark point that consistently yielded values for the neutrino oscillation parameters [59]. These values are listed in the second column of Table V for reference. The corresponding values of the mixing angles and mass-squared differences can be found in the second column of Table VI.

TABLE IV. The ranges of Yukawa couplings used in numerical analysis for normal and inverted hierarchies of neutrinos.

Yukawa coupling parameter	When $v_1 \ll v_2$ range		When v_1 ranges from (10–17) GeV range	
	NH	IH	NH	IH
b_{11}	$6 \times 10^{-2} - 8 \times 10^{-2}$	$7 \times 10^{-2} - 2 \times 10^{-1}$	$6 \times 10^{-2} - 8 \times 10^{-2}$	$8 \times 10^{-2} - 9 \times 10^{-2}$
b_{12}	$1 \times 10^{-2} - 5 \times 10^{-2}$	$2 \times 10^{-3} - 4 \times 10^{-3}$	$2 \times 10^{-2} - 3 \times 10^{-2}$	$2 \times 10^{-3} - 3 \times 10^{-3}$
b_{13}	$7 \times 10^{-1} - 9 \times 10^{-1}$	$3 \times 10^{-1} - 5 \times 10^{-1}$	$6 \times 10^{-1} - 8 \times 10^{-1}$	$1 \times 10^{-1} - 2 \times 10^{-1}$
b_{23}	$1 \times 10^{-4} - 5 \times 10^{-4}$	$4 \times 10^{-1} - 6 \times 10^{-1}$	$1 \times 10^{-3} - 2 \times 10^{-3}$	$4 \times 10^{-1} - 6 \times 10^{-1}$
b_{31}	$1 \times 10^{-4} - 5 \times 10^{-4}$	$3 \times 10^{-2} - 5 \times 10^{-2}$	$1 \times 10^{-2} - 2 \times 10^{-2}$	$3 \times 10^{-2} - 5 \times 10^{-2}$
b_{32}	$4 \times 10^{-2} - 6 \times 10^{-2}$	$3 \times 10^{-2} - 5 \times 10^{-2}$	$4 \times 10^{-2} - 6 \times 10^{-2}$	$6 \times 10^{-2} - 7 \times 10^{-2}$

TABLE V. The benchmark points yielding correct neutrino phenomenology (i.e., neutrino mixing angles and mass-squared differences are within 3σ experimental range [59]) for normal and inverted hierarchical neutrino masses.

Parameter (Units)	When $v_1 \ll v_2$		When v_1 ranges from (10–17) GeV	
	NH	IH	NH	IH
b_{11}	7.244577×10^{-2}	1.066963×10^{-1}	6.009812×10^{-2}	8.006565×10^{-2}
b_{12}	1.498695×10^{-2}	3.644816×10^{-3}	2.334813×10^{-2}	2.601354×10^{-3}
b_{13}	8.560231×10^{-1}	4.519143×10^{-1}	6.935666×10^{-1}	1.522807×10^{-1}
b_{23}	1.033423×10^{-4}	5.112375×10^{-1}	1.791234×10^{-3}	4.531115×10^{-1}
b_{31}	1.356340×10^{-4}	4.546001×10^{-2}	1.655557×10^{-2}	3.909223×10^{-2}
b_{32}	5.796197×10^{-2}	4.435139×10^{-2}	4.880238×10^{-2}	6.157254×10^{-2}
M_1 (GeV)	2.447917×10^{12}	6.721219×10^{12}	3.066113×10^{12}	4.417490×10^{12}
M_3 (GeV)	2.222544×10^{14}	5.140671×10^{14}	2.748449×10^{14}	6.211162×10^{14}

TABLE VI. The values of the neutrino oscillation parameters obtained using benchmark points given in Table V for normal and inverted hierarchical neutrino masses.

Parameters (Units)	When $v_1 \ll v_2$		When v_1 ranges from (10–17) GeV	
	NH	IH	NH	IH
θ_{13} ($^\circ$)	8.44	8.85	8.86	8.22
θ_{12} ($^\circ$)	31.70	34.30	32.10	31.80
θ_{23} ($^\circ$)	43.76	47.09	42.96	48.14
Δm_{21}^2 (eV^2)	7.61×10^{-5}	7.33×10^{-5}	7.64×10^{-5}	7.04×10^{-5}
Δm_{31}^2 (eV^2)	2.58×10^{-3}	2.48×10^{-3}	2.49×10^{-3}	2.43×10^{-3}

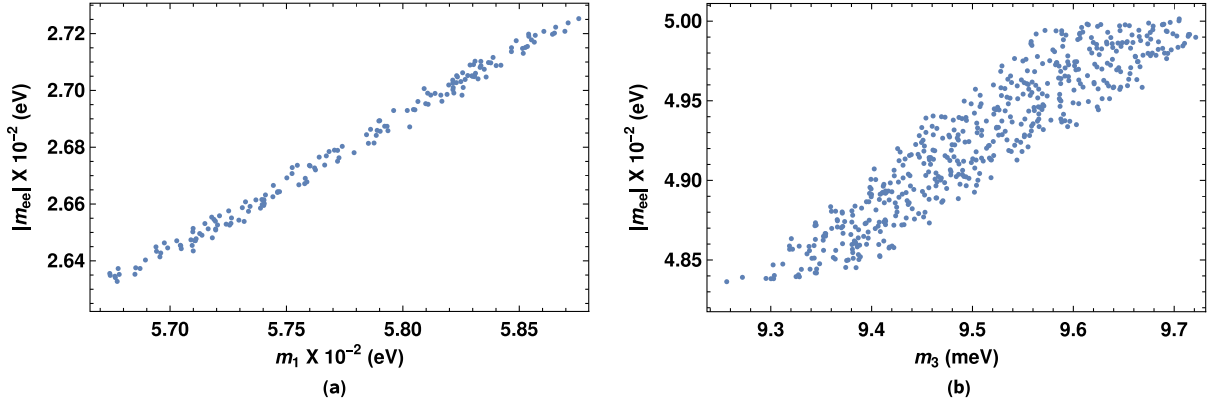


FIG. 1. Predictions for effective Majorana mass $|m_{ee}|$ for normal (left) and inverted (right) hierarchy when $v_1 \ll v_2$.

For these parameter values, the effective Majorana neutrino mass takes the values $|m_{ee}| = |\sum_i U_{ei}^2 m_i| = 0.02693$ eV and $|m_{ee}| = 0.04952$ eV for NH and IH of neutrinos, respectively. The masses m_1 , m_2 , and m_3 exhibited significant degeneracy in the case of NH, while for IH, there was an order of magnitude difference between the lightest mass and the other heavier masses. A linear correlation between $|m_{ee}|$ and the lightest neutrino mass (m_1 for NH and m_3 for IH) is evident in Fig. 1.

CP violation in the leptonic sector remains unobserved to date. Consequently, it will be instructive to scrutinize the model's predictions for CP violation. In our model, CP violation, effectively, seeds from the complex VEV $\langle \Phi_2 \rangle$ via its phase α . CP violation can be understood in a rephasing invariant way by defining Jarlskog parameter $J_{CP} = \Im(U_{\mu 3} U_{e 3}^* U_{e 2} U_{\mu 2}^*)$ [60–62]. For the present case, i.e., $v_1 \ll v_2$, we find that J_{CP} and δ (the phase of the $U_{e 3}$ element in U) are exceedingly small, regardless of the neutrino mass hierarchy and whether the VEV-phase α is equal to zero or nonzero (see Fig. 2). Figure 2 clearly illustrates that when $v_1 \ll v_2$, the model predicts a effective CP conserving scenario, regardless of the value of the VEV-phase α .

Furthermore, in this parameter space region, the mixing angle θ_{23} falls within the lower octant ($\theta_{23} < 45^\circ$) for the

normal hierarchy (NH) and the upper octant ($\theta_{23} > 45^\circ$) for the inverted hierarchy (IH), as illustrated in Fig. 3. Specifically, we note that the mixing angle θ_{23} is approximately 44° for the normal hierarchy and 47° for the inverted hierarchy. In the subsequent section, we will explore an alternative scenario by increasing the VEV v_1 to observe its impact on CP violation in the leptonic sector.

B. When VEV v_1 is in the GeV range

In this specific scenario, we randomly varied the VEV v_1 within the range of 10 to 17 GeV to analyze the influence of both VEVs on the parameter space. Once again, in this case, v_2 is determined by the relation $v_2 = \sqrt{v^2 - v_1^2}$ GeV. The predictions obtained for masses and other parameters will be discussed as follows.

1. Charged lepton masses

In this case, we have randomly varied the Yukawa couplings in range as shown in third column of Table I, and after diagonalizing the mass matrix $M_l M_l^\dagger$ numerically using Eq. (37), we have obtained squared-masses of the charged leptons. The benchmark point and prediction for the masses of charged leptons are listed in third column of Tables II and III, respectively.

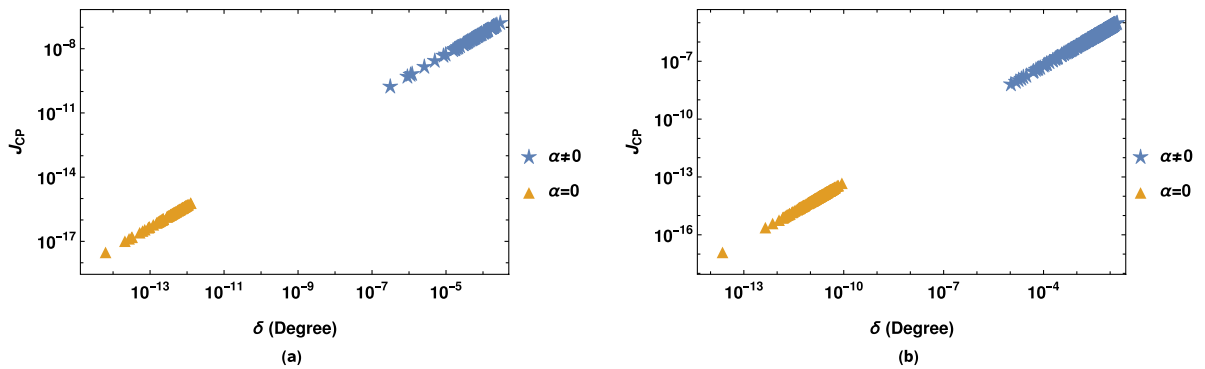


FIG. 2. $\delta - J_{CP}$ correlation with VEV-phase $\alpha = 0$ and $\alpha \neq 0$ for normal (left) and inverted (right) hierarchies.

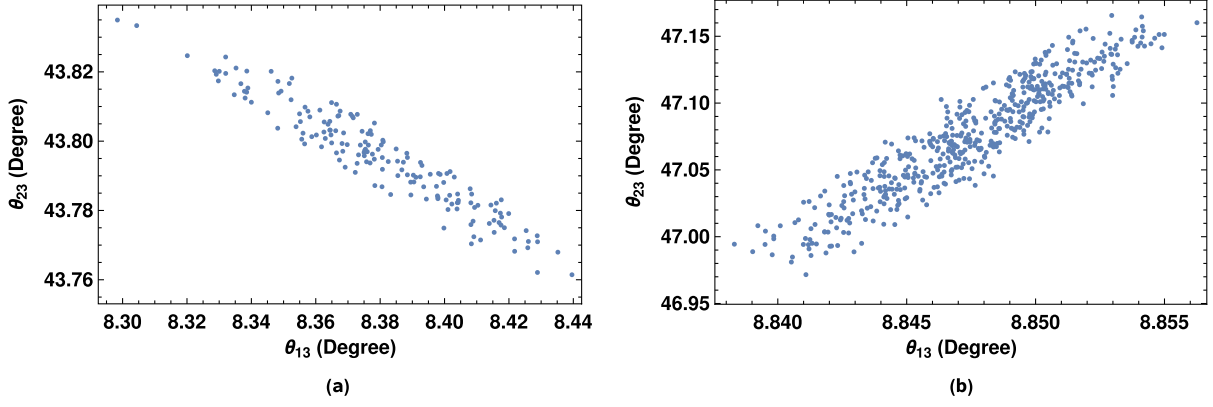


FIG. 3. Correlation between the mixing angles θ_{13} and θ_{23} for normal (left) and inverted (right) hierarchies.

2. Neutrino oscillation parameters

The ranges of Yukawa couplings considered in the numerical analysis are presented in the third column of Table IV. In both normal and inverted hierarchies of neutrinos, we have identified the benchmark point and obtained the values of the mixing angles and mass squared differences, as shown in the third column of Tables V and VI, respectively.

For these values, we have determined that $|m_{ee}|$ is approximately 0.01191 eV for NH and 0.04726 eV for

IH. Even with the increased value of v_1 , the masses m_1 , m_2 , and m_3 follow the same trend as in the previous case when $v_1 \ll v_2$.

The correlation plots, in Fig. 4, are shown for NH (first row) and IH (second row) cases. It can be seen from Fig. 4 that $|m_{ee}|$ is strongly correlated to m_1 [Fig. 4(a)] and Jarlskog invariant $J_{CP} \in (-0.006 \rightarrow 0.006)$ [Fig. 4(b)] for NH. For IH, $|m_{ee}| \in (4.67 \rightarrow 4.83) \times 10^{-2}$ eV [Fig. 4(c)] and $J_{CP} \in (-0.021 \rightarrow -0.018) \oplus (0.018 \rightarrow 0.021)$ [Fig. 4(d)].

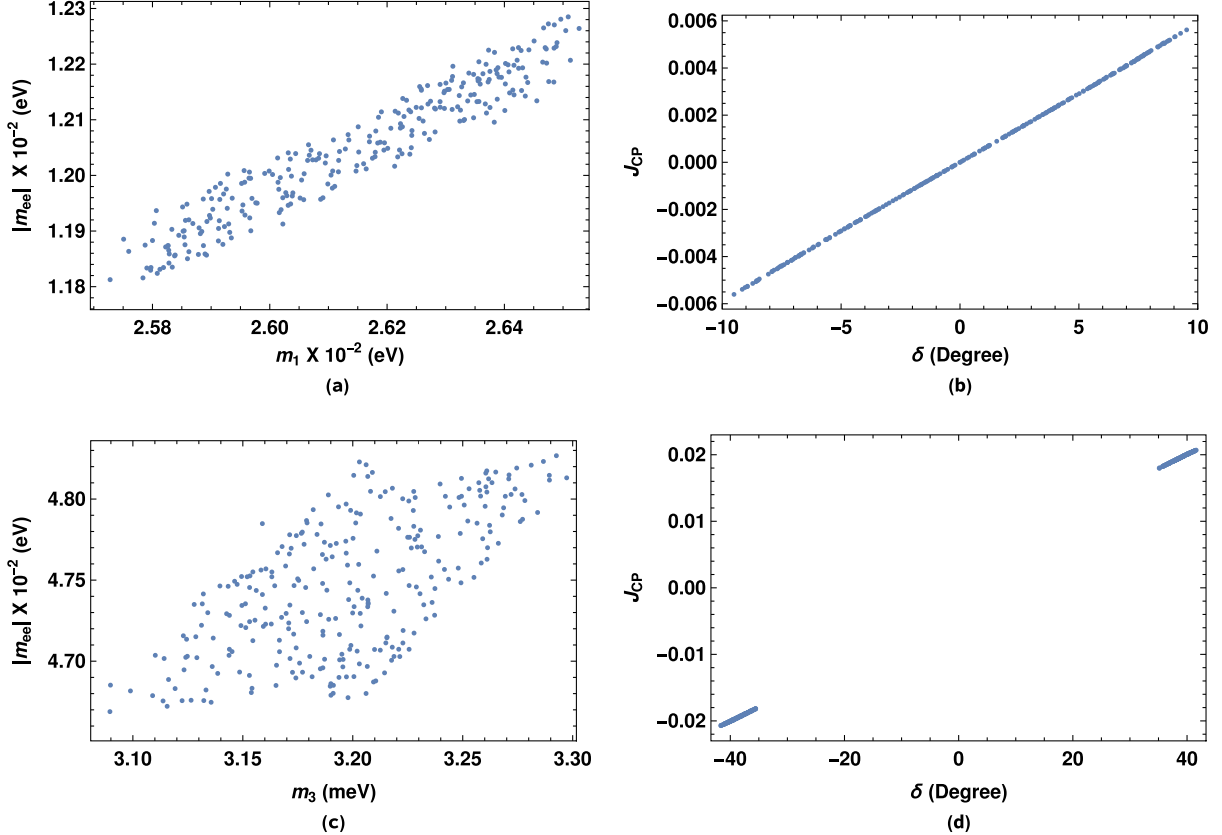
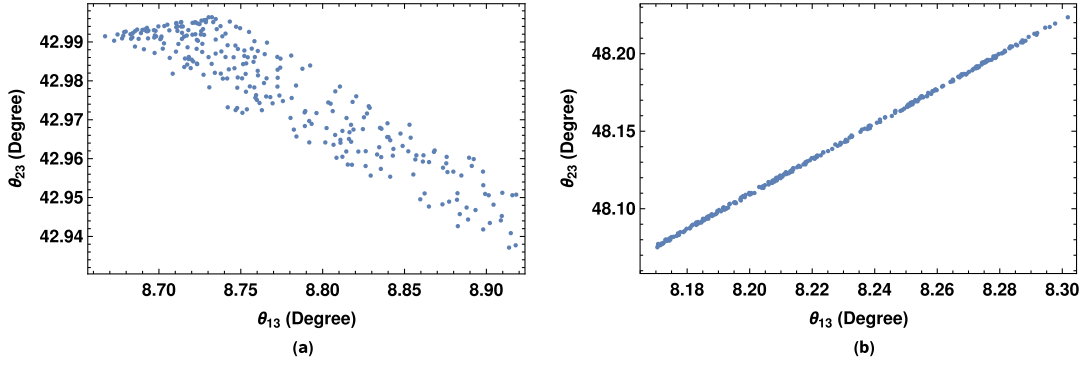
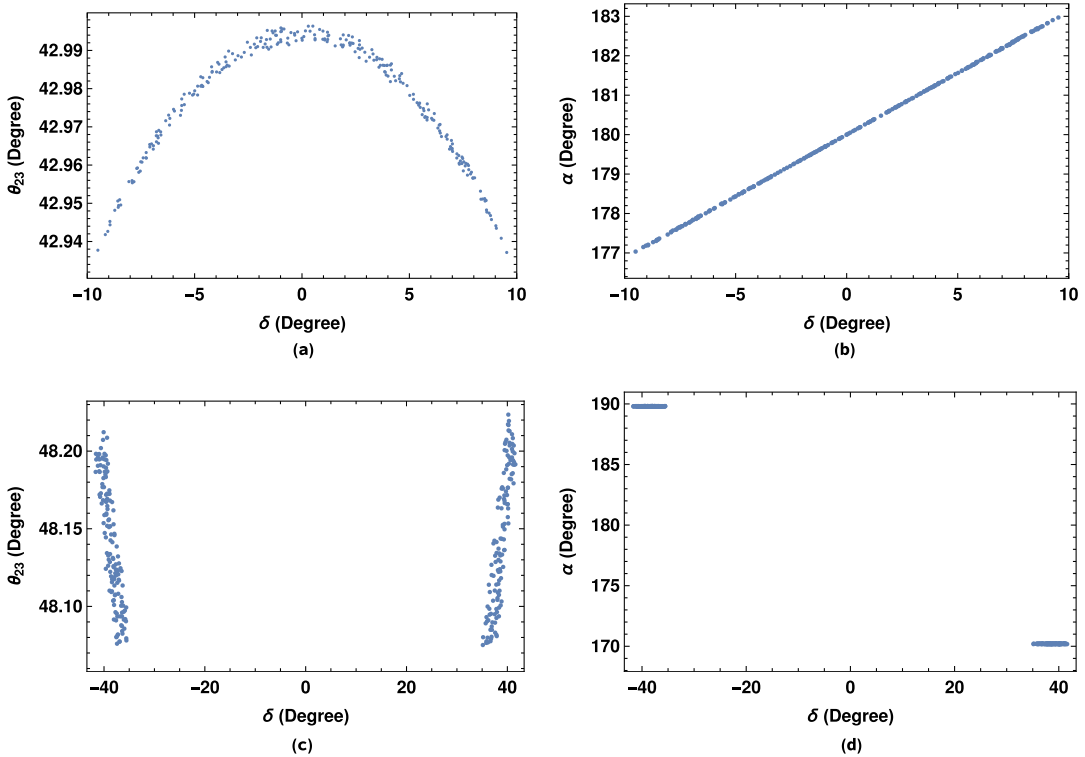


FIG. 4. Correlation plots between the effective neutrino mass $|m_{ee}|$ and lightest neutrino mass, as well as between J_{CP} and CP -violating phase δ , for both normal (first row) and inverted (second row) hierarchies when the VEV v_1 ranges from 10 to 17 GeV.


 FIG. 5. Correlation between the mixing angles θ_{13} and θ_{23} for normal (left) and inverted (right) hierarchies.

It is interesting to note that in case of IH, the CP violating phase $\delta = 0$ is disallowed, thus making this scenario necessarily CP violating. Another characteristic feature of the model is predicted correlation between yet unknown θ_{23} -octant and neutrino mass hierarchy. In Fig. 5, we have shown allo $(\theta_{13} - \theta_{23})$ plane. It is evident from these plots that, for NH (IH), mixing angles $(\theta_{13} - \theta_{23})$ exhibit negative (positive) correlation. Thus, θ_{23} resides in the lower octant for NH and in higher octant for IH; see Fig. 5. Further, the model exhibit a sharp prediction for θ_{23} approximately equal to 43° (48°) for NH (IH). Similarly, θ_{13} is found to be around 8.8° (8.24°) for NH (IH). The correlations predicted by the model between δ and (θ_{23}, α) , for NH and IH, are shown in Figs. 6(a)–6(d).

Multi-Higgs models often lead to significant flavor-changing neutral currents (FCNC) [63]. One approach to reduce these couplings is by aligning all right-handed fermions to interact with a single Higgs. This alignment can be achieved through an additional global Z_2 symmetry [12,13]. Alternatively, it can result from adjusting the ratio of the VEVs v_2/v_1 . In our study, we are investigating the consequences of generalized CP (GCP) symmetry without imposing additional symmetry constraints on the most general Yukawa couplings and their corresponding neutrino phenomenology. Within the model, it is possible that the Higgs responsible for FCNC is very heavy and thus produces vanishing FCNCs. The examination of FCNC effects in the current


 FIG. 6. Correlation of δ with θ_{23} and VEV-phase α for NH (first row) and IH (second row).

model is beyond the scope of this study and will be explored in future research.

In the present work, we have assumed the renormalization group evolution (RGE) effects on the parameters to be negligible. In fact, the literature extensively explores the impact of renormalization group (RG) effects on multiple Higgs doublet models. In Ref. [31], the authors have considered the impact of imposing generalized CP symmetries on the Higgs sector of the two-Higgs doublet model and identified three classes of symmetries ($CP1$, $CP2$, and $CP3$). They have, also, examined the vacuum structure and renormalization in the presence of these symmetries showing that the basis invariant condition (in their paper, $D = 0$), defining these symmetries, is RG invariant. Also, the effects of RGE have, also, been studied in Ref. [64] within two Higgs doublet models (considered in the present work). In particular, the authors have examined the RG equations of the quartic Higgs-potential parameters and found that the symmetries of this model are preserved by the RGEs. Furthermore, in Ref. [65], the authors investigated renormalization of the neutrino mass operators in the multi-Higgs-doublet. Considering representative models, they have shown that the corrections in the parameters are in general negligible, with the possible exception of a degenerate neutrino mass spectrum. In the present work, we, also, have obtained the mass spectrum to be hierarchical and not degenerate. Thus, we expect that RG effects to be negligible in our model as well.

V. CONCLUSIONS

In extended theoretical frameworks beyond the Standard Model, the count of free parameters increases compared to those at low energy. By introducing additional symmetry into the Lagrangian, we can substantially reduce the number of free parameters. In this study, we investigated the impact of GCP symmetries in the leptonic sector within the context of the 2HDM model. To incorporate nonzero neutrino masses, we have extended the lepton sector by introducing right-handed neutrinos through the Type-I seesaw mechanism.

The scalar potential of the 2HDM model typically involves 14 free parameters. However, due to the GCP

symmetry we impose, this number reduces to four in the unbroken $CP3$ case and six in the softly broken $CP3$ symmetry case. Consequent to GCP, the charged lepton [Eq. (13)] and neutrino Yukawa coupling [Eq. (14)] matrices contain 12 independent parameters, six each in charged lepton and neutrino sectors. Also, Majorana mass term have two real parameters [Eq. (30)].

This model exhibits a rich phenomenology and reveals strong correlations among neutrino oscillation parameters. The complex VEV phase α is the sole source of CP violation in the model. We consider two distinct phenomenological scenarios:

- (1) In the first scenario, where VEV v_1 is much smaller than v_2 , CP is conserved regardless of the value of the VEV-phase α (see Fig. 2). This scenario provides a unique phenomenology for normal and inverted hierarchies of neutrinos. Notably, the model precisely predicts the neutrino mixing angles, particularly the atmospheric mixing angle θ_{23} .
- (2) In the second scenario, where v_1 is in the GeV range, the atmospheric mixing angle θ_{23} is below (for NH) or above (for IH) maximality, approximately $\approx 43^\circ$ and $\approx 48^\circ$, respectively (see Fig. 5). The Dirac CP phase δ is tightly constrained to be within the range of -10° to 10° for the NH case. However, if the neutrino masses follow an inverted mass spectrum, the model inherently exhibits CP violation with δ approximately equal to $\pm 40^\circ$.

In summary, our investigation into the 2HDM model with GCP symmetries reduces the number of free parameters, leading to precise predictions for neutrino mixing angles and distinct CP -violating scenarios, shedding light on its unique phenomenology.

ACKNOWLEDGMENTS

Tapender acknowledges the financial support provided by Central University of Himachal Pradesh. The authors, also, acknowledge Department of Physics and Astronomical Science for providing necessary facility to carry out this work.

[1] P. Minkowski, *Phys. Lett.* **67B**, 421 (1977).
 [2] T. Yanagida, *Conf. Proc. C* **7902131**, 95 (1979).
 [3] S. L. Glashow, *NATO Sci. Ser. B* **61**, 687 (1980).
 [4] M. Gell-Mann, P. Ramond, and R. Slansky, *Conf. Proc. C* **790927**, 315 (1979).
 [5] R. N. Mohapatra and G. Senjanovic, *Phys. Rev. Lett.* **44**, 912 (1980).

[6] T. D. Lee, *Phys. Rev. D* **8**, 1226 (1973).
 [7] D. J. Castano, E. J. Piard, and P. Ramond, *Phys. Rev. D* **49**, 4882 (1994).
 [8] S. Weinberg, *Phys. Rev. Lett.* **40**, 223 (1978).
 [9] F. Wilczek, *Phys. Rev. Lett.* **40**, 279 (1978).
 [10] R. L. Workman *et al.* (Particle Data Group), *Prog. Theor. Exp. Phys.* **2022**, 083C01 (2022).

- [11] J. F. Gunion and H. E. Haber, *Phys. Rev. D* **67**, 075019 (2003).
- [12] S. L. Glashow and S. Weinberg, *Phys. Rev. D* **15**, 1958 (1977).
- [13] E. A. Paschos, *Phys. Rev. D* **15**, 1966 (1977).
- [14] R. D. Peccei and H. R. Quinn, *Phys. Rev. Lett.* **38**, 1440 (1977).
- [15] S. Antusch, M. Drees, J. Kersten, M. Lindner, and M. Ratz, *Phys. Lett. B* **525**, 130 (2002).
- [16] D. Atwood, S. Bar-Shalom, and A. Soni, *Phys. Lett. B* **635**, 112 (2006).
- [17] J. D. Clarke, R. Foot, and R. R. Volkas, *Phys. Rev. D* **92**, 033006 (2015).
- [18] Z. Liu and P. H. Gu, *Nucl. Phys.* **B915**, 206 (2017).
- [19] D. A. Camargo, M. D. Campos, T. B. de Melo, and F. S. Queiroz, *Phys. Lett. B* **795**, 319 (2019).
- [20] D. Cogollo, R. D. Matheus, T. B. de Melo, and F. S. Queiroz, *Phys. Lett. B* **797**, 134813 (2019).
- [21] L. Lopez Honorez, E. Nezri, J. F. Oliver, and M. H. G. Tytgat, *J. Cosmol. Astropart. Phys.* **02** (2007) 028.
- [22] M. Gustafsson, E. Lundstrom, L. Bergstrom, and J. Edsjo, *Phys. Rev. Lett.* **99**, 041301 (2007).
- [23] E. M. Dolle and S. Su, *Phys. Rev. D* **80**, 055012 (2009).
- [24] L. Lopez Honorez and C. E. Yaguna, *J. High Energy Phys.* **09** (2010) 046.
- [25] G. Arcadi, *Eur. Phys. J. C* **78**, 864 (2018).
- [26] E. Bertuzzo, S. Jana, P. A. N. Machado, and R. Zukanovich Funchal, *Phys. Lett. B* **791**, 210 (2019).
- [27] J. F. Gunion and H. E. Haber, *Phys. Rev. D* **72**, 095002 (2005).
- [28] M. Maniatis, A. von Manteuffel, and O. Nachtmann, *Eur. Phys. J. C* **57**, 739 (2008).
- [29] M. Maniatis and O. Nachtmann, *J. High Energy Phys.* **05** (2009) 028.
- [30] M. Maniatis and O. Nachtmann, *J. High Energy Phys.* **04** (2010) 027.
- [31] P. M. Ferreira, H. E. Haber, and J. P. Silva, *Phys. Rev. D* **79**, 116004 (2009).
- [32] P. M. Ferreira and J. P. Silva, *Eur. Phys. J. C* **69**, 45 (2010).
- [33] J. Velhinho, R. Santos, and A. Barroso, *Phys. Lett. B* **322**, 213 (1994).
- [34] I. P. Ivanov, *Phys. Rev. D* **75**, 035001 (2007); **76**, 039902(E) (2007).
- [35] M. Maniatis, A. von Manteuffel, O. Nachtmann, and F. Nagel, *Eur. Phys. J. C* **48**, 805 (2006).
- [36] C. C. Nishi, *Phys. Rev. D* **74**, 036003 (2006); **76**, 119901(E) (2007).
- [37] I. P. Ivanov, *Phys. Rev. D* **77**, 015017 (2008).
- [38] M. Maniatis, A. von Manteuffel, and O. Nachtmann, *Eur. Phys. J. C* **57**, 719 (2008).
- [39] M. Holthausen, M. Lindner, and M. A. Schmidt, *J. High Energy Phys.* **04** (2013) 122.
- [40] G. J. Ding, S. F. King, C. Luhn, and A. J. Stuart, *J. High Energy Phys.* **05** (2013) 084.
- [41] F. Feruglio, C. Hagedorn, and R. Ziegler, *J. High Energy Phys.* **07** (2013) 027.
- [42] C. C. Li and G. J. Ding, *Nucl. Phys.* **B881**, 206 (2014).
- [43] P. P. Novichkov, J. T. Penedo, S. T. Petcov, and A. V. Titov, *J. High Energy Phys.* **07** (2019) 165.
- [44] C. Y. Yao, J. N. Lu, and G. J. Ding, *J. High Energy Phys.* **05** (2021) 102.
- [45] J. Ganguly and R. S. Hundi, *Chin. Phys. C* **46**, 103101 (2022).
- [46] J. Ganguly, *Int. J. Mod. Phys. A* **37**, 2250095 (2022).
- [47] P. Chen, C. C. Li, and G. J. Ding, *Phys. Rev. D* **91**, 033003 (2015).
- [48] P. Chen, C. Y. Yao, and G. J. Ding, *Phys. Rev. D* **92**, 073002 (2015).
- [49] P. Chen, G. J. Ding, F. Gonzalez-Canales, and J. W. F. Valle, *Phys. Rev. D* **94**, 033002 (2016).
- [50] D. M. Barreiros, R. G. Felipe, and F. R. Joaquim, *J. High Energy Phys.* **01** (2019) 223.
- [51] N. Nath, R. Srivastava, and J. W. F. Valle, *Phys. Rev. D* **99**, 075005 (2019).
- [52] S. F. King, *Nucl. Phys. B, Proc. Suppl.* **95**, 261 (2001).
- [53] A. Abada, A. J. R. Figueiredo, J. C. Romao, and A. M. Teixeira, *J. High Energy Phys.* **10** (2010) 104.
- [54] A. Abada, A. J. R. Figueiredo, J. C. Romao, and A. M. Teixeira, *J. High Energy Phys.* **08** (2011) 099.
- [55] A. J. R. Figueiredo, *Eur. Phys. J. C* **75**, 99 (2015).
- [56] Y. K. Lei and C. Liu, *Commun. Theor. Phys.* **71**, 287 (2019).
- [57] M. A. Ouahid, M. A. Lualidi, R. A. Laamara, and E. H. Saïdi, *Phys. Rev. D* **102**, 115023 (2020).
- [58] G. Ecker, W. Grimus, and H. Neufeld, *J. Phys. A* **20**, L807 (1987).
- [59] P. F. de Salas, D. V. Forero, S. Gariazzo, P. Martínez-Miravé, O. Mena, C. A. Ternes, M. Tórtola, and J. W. F. Valle, *J. High Energy Phys.* **02** (2021) 071.
- [60] C. Jarlskog, *Phys. Rev. Lett.* **55**, 1039 (1985).
- [61] S. M. Bilenky and S. T. Petcov, *Rev. Mod. Phys.* **59**, 671 (1987); **61**, 169(E) (1989); **60**, 575(E) (1988).
- [62] P. I. Krastev and S. T. Petcov, *Phys. Lett. B* **205**, 84 (1988).
- [63] A. Crivellin, A. Kokulu, and C. Greub, *Phys. Rev. D* **87**, 094031 (2013).
- [64] M. Maniatis and O. Nachtmann, *J. High Energy Phys.* **11** (2011) 151.
- [65] W. Grimus and L. Lavoura, *Eur. Phys. J. C* **39**, 219 (2005).